

Determinants of Exercise-Induced Mitral Regurgitation Using Three-Dimensional Transesophageal Echocardiography Combined With Isometric Handgrip Exercise

Yu Harada, MD, Hiroto Utsunomiya, MD, PhD*, Hitoshi Susawa, MD, Kosuke Takahari, MD, Hajime Takemoto, MD, Yusuke Ueda, MD, Kanako Izumi, MD, Kiho Itakura, MD, Takayuki Hidaka, MD, PhD, and Yukiko Nakano, MD, PhD

Using three-dimensional (3D) transesophageal echocardiography (TEE) and isometric handgrip exercise (IHE), we investigated the determinants of exercise-induced mitral regurgitation (MR) according to MR etiologies. Seventy-six patients with more than moderate MR, 40 patients with functional MR (FMR) and 36 patients with degenerative MR (DMR), underwent 3D TEE combined with IHE. Mitral valve (MV) geometry and 3D vena contracta area (3D VCA) were simultaneously evaluated at baseline and during IHE. With regard to exercise-induced MR, Δ 3D VCA was calculated as the difference between 3D VCA at baseline and 3D VCA during IHE. IHE caused different changes in MV geometry between etiologies and led to exacerbation of 3D VCA at baseline. Larger Δ 3D VCA was observed in the FMR group compared with the DMR group ($15.9 \pm 10.3 \text{ mm}^2$ versus $7.3 \pm 4.2 \text{ mm}^2$; $p < 0.0001$). In multivariate analyses, tenting height and 3D VCA were selected as independent factors associated with Δ 3D VCA in the FMR group ($p = 0.0135$ and $p = 0.0201$, respectively), while flail width was selected as an independent factor associated with Δ 3D VCA in the DMR group ($p = 0.0066$). In conclusion, IHE alters mitral valve geometry and causes exacerbation of MR regardless of MR etiology and the determinants of exercise-induced MR differed between MR etiologies. © 2021 The Author(s). Published by Elsevier Inc. This is an open access article under the CC BY-NC-ND license (<http://creativecommons.org/licenses/by-nc-nd/4.0/>) (Am J Cardiol 2021;00:1–8)

Dynamic changes in mitral regurgitation (MR) during exercise are well-known as exercise-induced MR. When the exacerbation is severe, it is considered a prognosticator in heart failure (HF) patients.^{1,2} Exercise-stress echocardiography is an essential tool for diagnosis of exercise-induced MR. However, in previous studies, characterizations of the mechanisms for exercise-induced MR were hampered by several limitations of 2-dimensional (2D) transthoracic echocardiography (TTE) based quantitative assessment of mitral valve (MV) and MR.^{1–3} In contrast, with the development of 3-dimensional (3D) echocardiography and dedicated software analysis over the past decade, 3D transesophageal echocardiography (TEE) allows accurate measurement of the MV geometry and MR severity.^{4,5} Furthermore, isometric handgrip exercise (IHE) has long been reported as a useful method to differentiate patients with risk for HF among patient populations.⁶ In contrast to

dynamic load-testing (e.g., cycle exercise), it can be performed even during TEE. In this study, using 3D TEE combined with IHE, we sought to evaluate the changes in MV geometry and MR severity during exercise and to investigate the determinants of exercise-induced MR in functional MR (FMR) compared with degenerative MR (DMR).

Methods

We prospectively enrolled symptomatic patients with moderate or greater MR at baseline who underwent 3D TEE at Hiroshima University Hospital between May 2017 and July 2019. The patient population was divided into an FMR group and a DMR group based on pathogenic stratification by 2D TTE. The etiology of MR was defined as FMR if resulting from regional myocardial dysfunction or global remodeling of the LV in the presence of an anatomically normal valve apparatus, or as DMR if resulting from structural defects of the MV due to leaflet prolapse or flail. Patients with other degenerative alterations including rheumatic or sclerotic changes, or definite diagnosis of infective endocarditis were excluded. Patients with MV stenosis or previous valve surgery were also excluded. Informed consent was obtained from all participants and the study protocol was approved by our institutional ethics committee.

A comprehensive 2D TTE study was performed by experienced sonographers using a commercially available ultrasound system (EPIQ7 with S5-1 probe; Philips, Andover,

Department of Cardiovascular Medicine, Hiroshima University Graduate School of Biomedical and Health Sciences, Hiroshima, Japan. Manuscript received December 22, 2020; revised manuscript received and accepted April 13, 2021.

Sources of Funding: This work was partially supported by MSD Life Science Foundation, Public Interest Incorporated Foundation. This work was also supported by Takeda Science Foundation.

Disclosures: All authors have reported they have no relationships relevant to the contents of this paper to disclose.

*Corresponding author: Tel: (81) 82 257 5540; fax: (81) 82 257 1569.

E-mail address: hutsu@hiroshima-u.ac.jp (H. Utsunomiya).

MA). All measurements and recordings were performed according to the American Society of Echocardiography recommendations.⁷ LV end-diastolic volume, LV end-systolic volume, LV ejection fraction, and left atrial (LA) volume were calculated by the modified Simpson method using apical 2- and 4-chamber views.⁸ Systolic pulmonary artery pressure (SPAP) was calculated according to guidelines and right atrial pressure was estimated from the inferior vena cava diameter and respiratory changes.⁹ Severity of MR was graded comprehensively by an integrative approach using semiquantitative parameters and at least one quantitative parameter, including proximal isovelocity surface area-derived effective regurgitant orifice area, vena contracta width, regurgitant volume, and presence of systolic flow reversal in pulmonary veins according to the recommendations of the European Society of Cardiology and American Society of Echocardiography using three MR grades: mild, moderate, and severe.^{10,11} Regurgitant volume was calculated by the proximal isovelocity surface area method. Regurgitant fraction was determined by the regurgitant volume, while LV stroke volume was calculated as the difference between LV end-diastolic volume and LV end-systolic volume. In patients with atrial fibrillation, the parameters were calculated as means of 3 to 5 measurements.

3D TEE was performed using an EPIQ7 ultrasound system equipped with a matrix-array transducer that could display both 2D and 3D images (X7-2t or X8-2t Live 3D TEE transducer; Philips). All patients were administered an intravenous injection of diazepam and pentazocine for sedation during the 3D TEE examination. Volume datasets were obtained in the live 3D zoom mode (median frame rate: 17 Hz) or 6-beat full volume mode (median frame rate: 69 Hz) focusing on the MV. In addition, color Doppler live 3D zoom or 6-beat full volume datasets were acquired at the narrowest possible depth under breath-hold to obtain a higher volume rate (median frame rate: 35 Hz). In patients with atrial fibrillation or inability to hold their breath, the live 3D zoom mode with 1-beat volume acquisition was chosen. The live 3D zoom or full volume datasets were digitally stored for off-line analysis and imported into a QLAB workstation (version 10.7; Philips).

Just before the 3D TEE examination, maximal voluntary contraction (MVC) was measured in all patients using the handgrip diameter. During 3D TEE, all patients were administered sedative drugs intermittently according to their level of sedation. After 3D volume data acquisition at baseline for offline analysis, drug administration was stopped to control patient awakening. In the final TEE examination, patients used their dominant hand to perform 3 minutes of IHE at 30% MVC in a left lateral decubitus position. Systolic blood pressure (BP), diastolic BP, and heart rate were measured using an automated brachial artery BP cuff (BMS-1763; Nihon Kohden, Tokyo, Japan). Finally, hemodynamic status and 3D volume data focused on the MV were carefully recorded for the final minute of IHE.

All 3D volume datasets were analyzed offline using the QLAB mitral valve navigation (MVN) and 3D quantification (3DQ) software package (Philips). Regarding the timing for assessment of 3D MV geometry and 3D VCA, the

occurrence of the peak velocity in the corresponding continuous wave Doppler signals was used for orientation. In all FMR patients, the mid-systolic frame was selected, while in 17 DMR patients (38%), the mid-to-late systolic frame was selected. The QLAB MVN software semi-automatically tracked the landmarks in a specified frame to create a 3D mitral model. After approval of the tracking, the software provided several 3D measurements of the MV geometry: anterolateral-posteromedial (AL-PM) diameter, anterior-posterior (A-P) diameter, annular area, annular height, tenting height, tenting volume, prolapse height, and prolapse volume (Figure 1 A–H).⁴ Furthermore, in all DMR patients, a cross-sectional plane through the MV leaflets was selected and the maximum flail gap and width were measured with movement of the 2D planes in the 3D space at the same frame (Figure 1 I and J). All measurements were acquired at baseline and during IHE with specified timing of the systolic phase.

By quantitative analysis of 3D color Doppler data, the 3D VCA was derived through three multiplanar reconstruction planes in a specified frame. After the two orthogonal long-axis planes were aligned parallel with the direction of the proximal MR jet, the short-axis plane was aligned perpendicular to the narrowest neck of the MR jet just above the left atrial side of the flow convergence zone. The resultant short-axis image of the MR jet was manually traced to obtain the 3D VCA.⁵ The three multiplanar reconstruction planes of the regurgitant jet, 3D color MV image, and measured 3D VCA in each FMR and DMR patient are shown in Figure 2. 3D VCA was measured at baseline and during IHE in all patients. Δ 3D VCA was defined as the change in 3D VCA during exercise and calculated by the difference between 3D VCA at baseline and 3D VCA during IHE.

Statistical analyses were performed with JMP ver. 14.0 software (SAS Institute Inc., Cary, NC). Continuous variables were expressed as median (25th and 75th percentiles) or mean \pm standard deviation (SD). Groups comparisons were performed by Student's t-test. A paired t-test was used to compare hemodynamic status and MV geometry at rest and during IHE. Comparisons of the effects of IHE on MV geometry between the groups were carried out by two-way ANOVA for repeated measures. Correlations between peak Vo_2 and Δ 3D VCA in the FMR and DMR groups were assessed by Pearson correlation coefficients and linear regression analysis. Multivariate stepwise linear regression analysis was performed to identify contributing factors related to Δ 3D VCA in the FMR and DMR groups, and significant variables in the univariate analyses were entered into the models. The following potential univariate predictors at baseline were initially considered for the analysis: systolic BP, diastolic BP, heart rate, AL-PM diameter, A-P diameter, annular area, annular height, tenting height, tenting volume, prolapse height, prolapse volume, flail gap, flail width, and baseline 3D VCA. For reproducibility, 3D TEE measurements, as described by absolute differences with SDs and intraclass correlations, were analyzed in a randomly selected sample of 40 datasets in MR patients (20 FMR patients and 20 DMR patients). The selected datasets were evaluated at 1 month after the initial measurement by the first author for intra observer variability and by a second

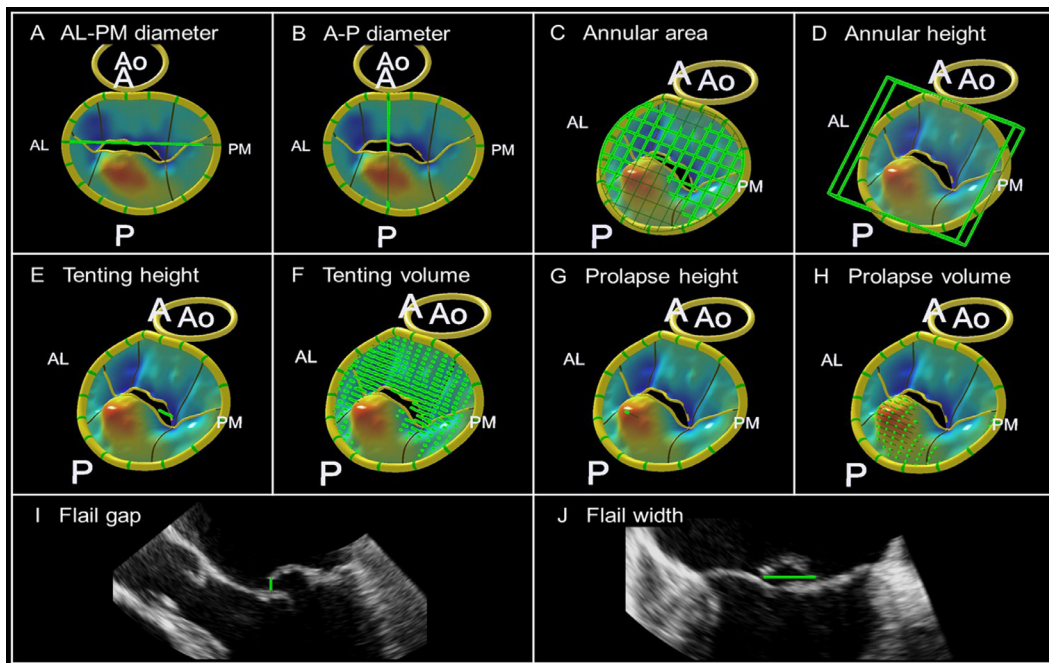


Figure 1. 3D parameters of MV geometry. (A–H) After approval of the tracking, the MVN software semi-automatically creates a 3D mitral model and provides 3D parameters of the MV. (I, J) In patients with degenerative MR, flail gap (I) and flail width (J) are searched and measured at their maximum length in a cross-sectional plane through the MV leaflets. 3D = three-dimensional; MV = mitral valve; MR = mitral regurgitation; MV = mitral valve.

observer for interobserver variability. Two-sided values of $p < 0.05$ were considered statistically significant.

Results

A total of 76 patients were enrolled in the study. The FMR group consisted of 40 patients comprising 17 dilated cardiomyopathy, 10 ischemic cardiomyopathy, and 13 atrial MR, while the DMR group consisted of 36 patients comprising 21 leaflet prolapse and 15 leaflet flail. The clinical and TTE parameters in the two MR groups are summarized

in Table 1. In the 2D TTE parameters, the FMR group had significantly larger LV end-diastolic volume, LV end-systolic volume, and lower LV ejection fraction (all $p < 0.001$) with larger LA volume. As for MR severity, both regurgitant volume and fraction were similar in the two groups (Table 1).

The hemodynamic status and 3D parameters of MV geometry in the two MR groups at baseline and during IHE are summarized in Table 2. In the baseline 3D parameters of MV geometry, AL-PM diameter, A-P diameter, annular area, and annular height also showed no significant

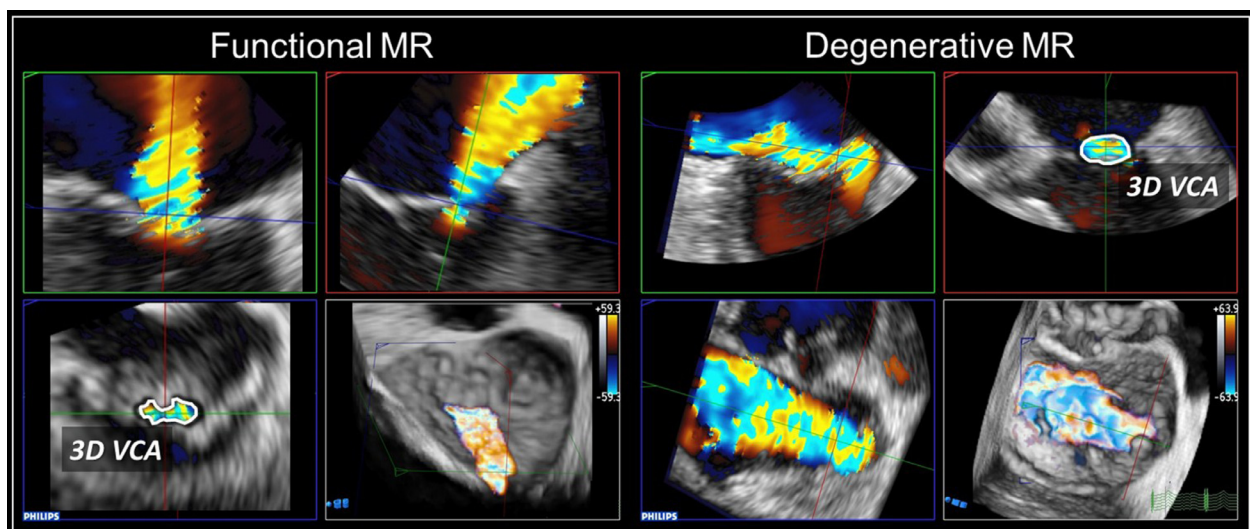


Figure 2. . Examples of 3D VCA quantitative analysis in functional MR and degenerative MR. Using acquired 3D color Doppler MV data, the QLAB 3DQ software can display three orthogonal planes of the regurgitant jet and a 3D MV image. After the two orthogonal long-axis planes are set with the direction of the regurgitant jet, 3D VCA is obtained by the short-axis plane at the narrowest neck region of the regurgitant jet (white circles). VCA = vena contracta area. Other abbreviations as Figure 1.

Table 1
Clinical and echocardiographic characteristics

Variable	Functional MR (n = 40)	Degenerative MR (n = 36)	p
Age (years)	71 (61–77)	68 (60–74)	0.96
Men	25 (63%)	22 (61%)	0.90
Body surface area (m ²)	1.61 (1.46–1.72)	1.59 (1.43–1.77)	0.63
Atrial fibrillation	13 (33%)	3 (8%)	0.02
Hypertension	29 (73%)	18 (50%)	0.04
Left ventricular end-diastolic volume (mL)	140 (105–201)	111 (81–136)	< 0.001
Left ventricular end-systolic volume (mL)	89 (56–134)	39 (31–46)	< 0.001
Left ventricular ejection fraction (%)	36 (28–48)	66 (62–69)	< 0.001
Left atrial volume (mL)	100 (76–132)	85 (64–110)	0.046
Systolic pulmonary artery pressure (mm Hg)	36 (29–49)	34 (27–40)	0.40
Severe mitral regurgitation	23 (58%)	27 (75%)	0.11
Regurgitant volume (mL)	44 (32–56)	61 (44–75)	0.22
Regurgitant fraction (%)	47 (42–64)	51 (44–57)	0.81

Data are shown as median (interquartile range) or n (%).

differences. The FMR group had higher tenting height and larger tenting volume than the DMR group (both $p < 0.0001$). In contrast, the DMR group had higher prolapse height and larger prolapse volume than the FMR group (both $p < 0.0001$). IHE elevated the baseline systolic BP, diastolic BP, and heart rate in both MR groups (all $p < 0.001$). The changes in systolic BP and heart rate did not differ significantly between the two groups, whereas the changes in diastolic BP were larger in the DMR group compared with the FMR group (Table 2). In the FMR group, significant augmentations in tenting height and tenting volume were observed during IHE (both $p < 0.001$). Meanwhile, in the DMR group, significant reductions in annular

height and tenting volume were observed during IHE (both $p < 0.02$). Furthermore, significant augmentations in prolapse height, prolapse volume, flail gap, and flail width were observed in the DMR group (Table 2).

Representative 3D color Doppler images of the MV and MR at baseline and during IHE in both MR groups are shown in the upper panels in Figure 3A and 3B. Different mitral models in each phase analyzed by the MVN software are shown in the lower panels of Figure 3A and 3B.

Figure 4 shows the changes in 3D VCA caused by IHE. In our study, baseline 3D VCA in the FMR group was smaller than that in the DMR group ($36.7 \pm 17.5 \text{ mm}^2$ vs $46.4 \pm 19.0 \text{ mm}^2$; $p = 0.022$). IHE caused significant exacerbations of baseline 3D VCA in both MR groups (FMR: $36.7 \pm 17.5 \text{ mm}^2$ to $52.6 \pm 24.0 \text{ mm}^2$; DMR: $46.4 \pm 19.0 \text{ mm}^2$ to $53.8 \pm 21.1 \text{ mm}^2$; both $p < 0.0001$). Despite the presence of smaller 3D VCA at baseline, the FMR group had larger $\Delta 3D$ VCA than the DMR group ($15.9 \pm 10.3 \text{ mm}^2$ vs $7.3 \pm 4.2 \text{ mm}^2$; $p < 0.0001$).

As shown in Table 3, univariable analyses revealed that tenting height, tenting volume, and baseline 3D VCA were significantly correlated with $\Delta 3D$ VCA in the FMR group. Meanwhile, AL-PM diameter, prolapse height, prolapse volume, flail gap, flail width, and baseline 3D VCA were significantly correlated with $\Delta 3D$ VCA in the DMR group. When these univariable determinants were entered into the multivariable stepwise linear regression analysis, tenting height ($p = 0.014$) and baseline 3D VCA ($p = 0.02$) were selected as independent predictors of $\Delta 3D$ VCA in the FMR group, whereas only flail width ($p = 0.007$) was selected as an independent predictor of $\Delta 3D$ VCA in the DMR group.

The intra observer and interobserver variabilities of the 3D TEE datasets were 1.9 ± 1.4 and $2.4 \pm 1.9 \text{ mm}$ for 3D measurements of MV geometry and 2.5 ± 1.7 and $3.2 \pm 2.4 \text{ mm}^2$ for 3D VCA, respectively. The intraclass

Table 2
Impacts of isometric handgrip exercise on hemodynamic status and 3D mitral valve geometry

Variable	Functional MR (n = 40)		Degenerative MR (n = 36)		p (time- group interaction)
	Baseline	Handgrip	Baseline	Handgrip	
Hemodynamic status					
Systolic blood pressure (mm Hg)	122 ± 28	138 ± 32*	131 ± 19	149 ± 19*	0.51
Diastolic blood pressure (mm Hg)	74 ± 18	83 ± 18*	78 ± 12	94 ± 13*,†	0.01
Heart rate (bpm)	77 ± 17	84 ± 16*	72 ± 12	80 ± 12*	0.73
3D mitral valve geometry					
AL-PM diameter (mm)	39.6 ± 5.8	39.6 ± 5.9	39.2 ± 4.2	39.5 ± 4.4	0.23
A-P diameter (mm)	31.9 ± 5.2	31.7 ± 5.2	31.4 ± 4.2	31.8 ± 4.1	0.14
Annular area (100 mm ²)	10.5 ± 3.1	10.3 ± 3.1	10.2 ± 2.3	10.3 ± 2.4	0.08
Annular height (mm)	4.3 ± 1.3	4.1 ± 1.3	3.8 ± 1.1	3.4 ± 0.7*,†	0.36
Tenting height (mm)	8.8 ± 2.6	9.3 ± 2.6*	6.0 ± 1.9†	5.8 ± 1.9†	< 0.001
Tenting volume (mL)	3.8 ± 1.7	4.1 ± 1.8*	1.5 ± 0.9†	1.4 ± 0.9*,†	< 0.001
Prolapse height (mm)	0.3 ± 0.7	0.2 ± 0.7	3.9 ± 2.1†	4.6 ± 2.2*	< 0.001
Prolapse volume (mL)	0.0 ± 0.0	0.0 ± 0.0	0.5 ± 0.5†	0.6 ± 0.7*	< 0.001
Flail gap (mm)	N/A	N/A	3.7 ± 1.5	4.0 ± 1.9*	N/A
Flail width (mm)	N/A	N/A	11.2 ± 3.1	11.6 ± 3.2*	N/A

Data are shown as mean ± SD.

* $p < 0.05$ versus baseline.

† $p < 0.05$ versus functional MR.

AL-PM, anterolateral-posteromedial; A-P, antero-posterior.

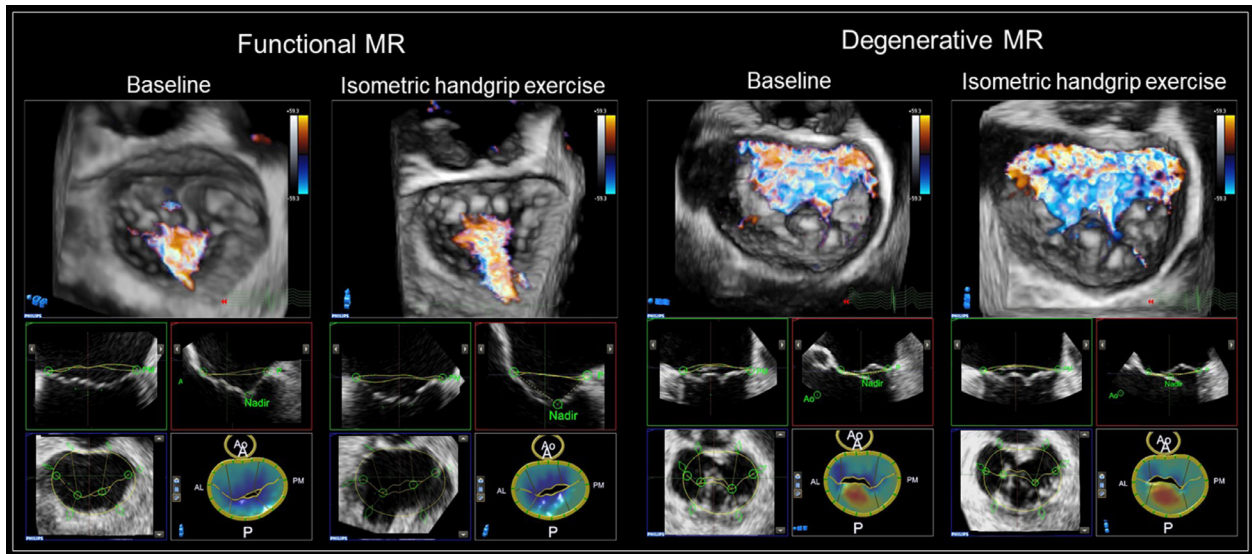


Figure 3. . Representative cases of IHE-stress 3D TEE. (Upper) 3D color MV images at baseline and during IHE in both MR groups (left, functional MR; right, degenerative MR). (Lower) 3D MV geometry analyzed by the MVN software at baseline and during IHE in both MR groups (left, functional MR; right, degenerative MR). Note that exacerbation of the MR jet and the changes in MV geometry occur concomitantly during IHE. IHE = isometric handgrip exercise. Other abbreviations as Figure 1.

correlations (95% confidence intervals) were 0.94 (0.92–0.96) and 0.93 (0.91–0.95) for 3D measurements of MV geometry and 0.92 (0.90–0.95) and 0.90 (0.86–0.93) for 3D VCA, respectively.

Discussion

To date, several studies using 2D TTE with cycle exercise have shown that exercise-induced MR was associated with acute pulmonary edema, exercise intolerance, and poor prognosis regardless of the MR etiology.^{1,3,12,13} Indeed, exercise-stress echocardiography

has proven to be a strong prognostic indicator in patients with unexplained dyspnea and may be useful for classification of heart failure with preserved LV ejection fraction.^{14,15} Thus, the current guidelines of the American Society of Echocardiography and European Association of Echocardiography recommend 2D TTE with cycle ergometer exercise for general diastolic stress testing.^{16,17} However, compared with TEE, it is well known that TTE has several clinical limitations to its application from the perspective of imaging quality. For example, obesity, poor acoustic window limited by respiratory excursion, and motion artifacts impair the

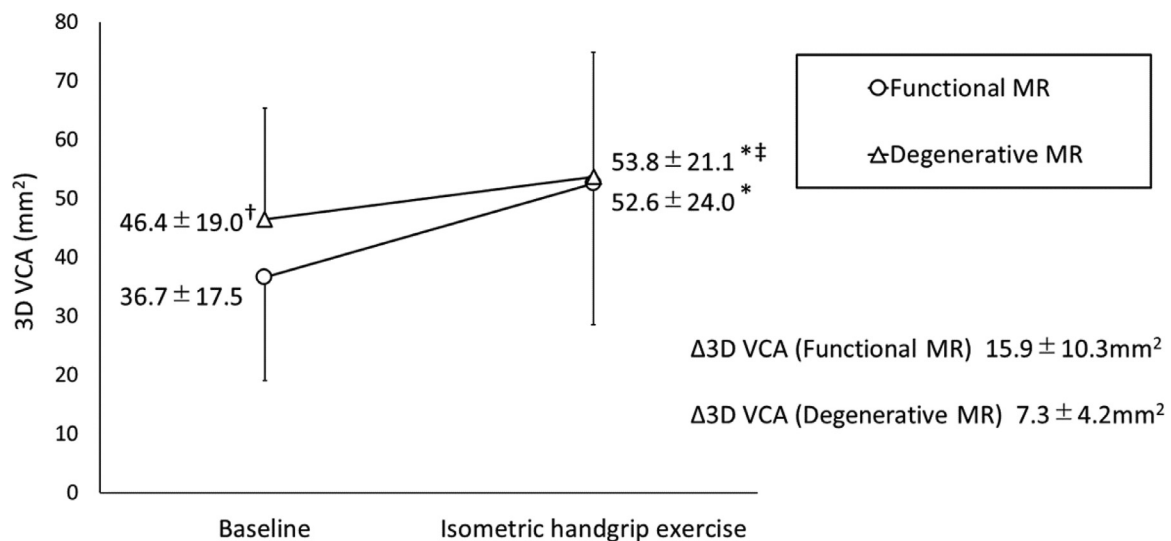


Figure 4. Changes in 3D VCA during IHE in the two MR groups. IHE significantly increases baseline 3D VCA in both MR groups (circles, functional MR; triangles, degenerative MR), but larger Δ 3D VCA is observed in the functional MR group compared with the degenerative MR group ($p < 0.0001$). * $p < 0.0001$ versus baseline, † $p = 0.022$ versus functional MR, ‡ $p = 0.82$ versus functional MR. IHE = isometric handgrip exercise. Other abbreviations as Figures 1 and 2.

Table 3

Correlations and associations of baseline hemodynamic status and 3D mitral valve geometry with Δ 3D vena contracta area during isometric handgrip exercise

Functional MR	Univariable		Multivariable				
	r	p	B	β	95% CI	p	VIF
Tenting height	0.47	0.002	1.456	0.366	0.318-2.593	.014	1.098
Tenting volume (per 0.1 mL)	0.28	0.079					
Baseline 3D vena contracta area	0.45	0.003	0.202	0.343	0.034-0.371	.02	1.098
Degenerative MR	Univariable		Multivariable				
	r	p	B	β	95% CI	p	VIF
AL-PM diameter	0.29	0.088					
Prolapse height	0.36	0.029					
Prolapse volume (per 0.1 mL)	0.34	0.044					
Flail gap	0.39	0.020					
Flail width	0.44	0.007	0.611	0.445	0.182-1.039	.007	1.000
Baseline 3D vena contracta area	0.41	0.013					

β , standardized regression coefficient; CI, confidence interval; VIF, variance inflation factor.

measurement accuracy for MV geometry and quantitative MR.^{18,19} Furthermore, these limitations are known to be exacerbated by cycle exercise, even at low intensity. In contrast, 3D TEE combined with IHE makes it possible to obtain accurate parameters of MV geometry and 3D VCA without such limitations. The present study substantiates the hypotheses suggested by several prior studies, highlighting the putative value of 3D echocardiography-based evaluation of the mechanisms of exercise-induced MR. The main findings in the present cohort of symptomatic patients with moderate or greater MR were: (1) IHE alters MV geometry and causes exacerbation of 3D VCA regardless of MR etiology; and (2) the factors associated with Δ 3D VCA differ between FMR and DMR.

With regard to changes in MV geometry during IHE, the present study showed that IHE in the FMR group significantly increased tenting height and volume with no annular parametrical changes. Overt heart failure symptoms frequently occur in FMR because of LV dysfunction and remodeling. It has been presumed that exercise-induced MR in FMR is caused by increased tethering force in the MV, which is affected by various components during exercise, including LV geometry (size and sphericity), dys-synchrony, and induced myocardial ischemia.^{20,21} Although changes in LV geometry were not evaluated in this study, we believe that increased LV afterload during IHE altered LV geometry and then increased the tethering force in the MV. Meanwhile, the MV geometry response during IHE in the DMR group was entirely different, comprising decreases in annular height, tenting height, and tenting volume, and increases in prolapse height, prolapse volume, flail gap, and flail width. No significant changes in AL-PM diameter, A-P diameter, and annular area were observed during IHE in the DMR group, similar to the FMR group. In DMR, therefore, the increase in LV afterload during IHE may contribute to compression of the MV toward the left atrium, followed by augmentation of the extent of leaflet prolapse. The newly advocated exercise test, IHE-stress 3D TEE, demonstrated these MV geometrical changes and their association with increases in 3D VCA, suggesting

different mechanisms for exercise-induced MR according to its etiology.

In this study, tenting height and baseline 3D VCA were selected as multivariable determinants of exercise-induced MR in patients with FMR, whereas only flail width was selected in patients with DMR. Therefore, even if non-severe MR is observed on resting echocardiography, patients with clinically significant MR who have effort dyspnea in daily life or are hospitalized for worsening heart failure should be suspicious for MR exacerbation upon exercise, especially among FMR patients with large tenting height and baseline 3D VCA and DMR patients with large flail width. Furthermore, transient increases in MR during exercise may accelerate progression of LV remodeling and/or valvular degeneration, which can trigger further deformation of the MV with greater extents of leaflet tethering and/or prolapse. Our findings establish the determinants of exercise-induced MR differed between MR etiologies, and highlight the importance for simultaneous assessment of MR severity and MV geometry during exercise in heart failure patients with moderate or greater MR.

There were some limitations in this study. This was a single-center study. Because of the small number of patients in the study population, the strength of the imaging variables for incremental addition to determine exercise-induced MR is uncertain. Further validation in a larger multicenter study is required to confirm our findings. Second, the changes in the LV and atrial geometry, which may help differentiate atrial from ventricular FMR and the IHE-induced pathophysiology of atrial vs ventricular FMR, were not evaluated in this study. Finally, we selected patients with MR based on the presence of leaflet prolapse or flail leaflet as DMR. Therefore, our findings cannot be applied to patients with other degenerative alterations, such as rheumatic or sclerotic changes, infective endocarditis.

Authors' Statement

List of all Authors: Yu Harada, Hiroto Utsunomiya, Hitoshi Susawa, Kosuke Takahari, Hajime Takemoto, Yusuke Ueda, Kanako Izumi, Kiho Itakura, Takayuki

Hidaka, Yukiko Nakano. Corresponding Author: Hiroto Utsunomiya

The corresponding author is responsible for ensuring that the descriptions are accurate and agreed by all authors. The roles of all authors in this manuscript is listed as follows:

- 1 Yu Harada: Visualization, Investigation, and Writing – original draft preparation.
- 2 Hiroto Utsunomiya: Conceptualization, Methodology, Funding acquisition, and Writing – review & editing.
- 3 Hitoshi Susawa: Investigation.
- 4 Kosuke Takahari: Validation.
- 5 Hajime Takemoto: Investigation.
- 6 Yusuke Ueda: Investigation.
- 7 Kanako Izumi: Investigation.
- 8 Kiho Itakura: Formal Analysis.
- 9 Takayuki Hidaka: Project administration.
- 10 Yukiko Nakano: Project administration and Supervision.

Conflict of Interest Statement

This statement is to certify that all authors have seen and approved the manuscript being submitted, have contributed significantly to the work, attest to the validity and legitimacy of the data and its interpretation, and agree to its submission to *The American Journal of Cardiology*.

We attest that the article is the Authors' original work, has not received prior publication and is not under consideration for publication elsewhere.

On behalf of all Co-Authors, the corresponding Author shall bear full responsibility for the submission. Any changes to the list of authors, including changes in order, additions or removals will require the submission of a new author agreement form approved and signed by all the original and added submitting authors.

All authors are requested to disclose any actual or potential conflict of interest including any financial, personal or other relationships with other people or organizations within three years of beginning the submitted work that could inappropriately influence, or be perceived to influence, their work. If there are no conflicts of interest, the COI should read: "The authors report no relationships that could be construed as a conflict of interest".

Acknowledgments

We would like to thank Hiroshi Ofuji and Takayuki Hataoka from Philips Electronics Japan for their technical assistance. We also thank Alison Sherwin, PhD, from Edanz Group (<https://en-author-services.edanzgroup.com/>) for editing a draft of this manuscript.

1. Lancellotti P, Troisfontaines P, Toussaint A, Pierard LA. Prognostic importance of exercise-induced changes in mitral regurgitation in patients with chronic ischemic left ventricular dysfunction. *Circulation* 2003;108:1713–1717.
2. Lancellotti P, Gérard PL, Piérard LA. Long-term outcome of patients with heart failure and dynamic functional mitral regurgitation. *Eur Heart J* 2005;26:1528–1532.
3. Magne J, Lancellotti P, Piérard LA. Exercise-induced changes in degenerative mitral regurgitation. *J Am Coll Cardiol* 2010;56:300–309.
4. Lee APW, Hsiung MC, Salgo IS, Fang F, Xie JM, Zhang YC, Lin QS, Looi JL, Wan S, Wong RHL, Underwood MJ, Sun JP, Yin WH, Wei J, Tsai SK, Yu CM. Quantitative analysis of mitral valve morphology in mitral valve prolapse with real-time 3-dimensional echocardiography: Importance of annular saddle shape in the pathogenesis of mitral regurgitation. *Circulation* 2013;127:832–841.
5. Thavendiranathan P, Phelan D, Collier P, Thomas JD, Flamm SD, Marwick TH. Quantitative assessment of mitral regurgitation. *JACC Cardiovasc Imaging* 2012;5:1161–1175.
6. Samuel TJ, Beaudry R, Haykowsky MJ, Sarma S, Nelson MD. Diastolic stress testing: similarities and differences between isometric handgrip and cycle echocardiography. *J Appl Physiol* 2018;125:529–535.
7. Kehl DW, Rader F, Siegel RJ. Echocardiographic features and clinical outcomes of flail mitral leaflet without severe mitral regurgitation. *J Am Soc Echocardiogr* 2017;30:1162–1168.
8. Lang RM, Badano LP, Mor-Avi V, Afilalo J, Armstrong A, Ernande L, Flachskampf FA, Foster E, Goldstein SA, Kuznetsova T, Lancellotti P, Muraru D, Picard MH, Rietzschel ER, Rudski L, Spencer KT, Tsang W, Voigt JU. Recommendations for cardiac chamber quantification by echocardiography in adults: An update from the American society of echocardiography and the European association of cardiovascular imaging. *Eur Heart J Cardiovasc Imaging* 2015;16:233–271.
9. Rudski LG, Lai WW, Afilalo J, Hua L, Handschumacher MD, Chandrasekaran K, Solomon SD, Louie EK, Schiller NB. Guidelines for the echocardiographic assessment of the right heart in adults: a report from the American Society of Echocardiography. *J Am Soc Echocardiogr* 2010;23:685–713.
10. Lancellotti P, Tribouilloy C, Hagendorff A, Popescu BA, Edvardsen T, Pierard LA, Badano L, Zamorano JL. Recommendations for the echocardiographic assessment of native valvular regurgitation: an executive summary from the European Association of Cardiovascular Imaging. *Eur Hear J - Cardiovasc Imaging* 2013;14:611–644.
11. Zoghbi WA, Adams D, Bonow RO, Enriquez-Sarano M, Foster E, Grayburn PA, Hahn RT, Han Y, Hung J, Lang RM, Little SH, Shah DJ, Sherman S, Thavendiranathan P, Thomas JD, Weissman NJ. Recommendations for noninvasive evaluation of native valvular regurgitation. *J Am Soc Echocardiogr* 2017:1–69.
12. Piérard LA, Lancellotti P. The role of Ischemic mitral regurgitation in the pathogenesis of acute pulmonary edema. *N Engl J Med* 2004;351:1627–1634.
13. Utsunomiya H, Hidaka T, Susawa H, Izumi K, Harada Y, Kinoshita M, Itakura K, Masada K, Kihara Y. Exercise-stress echocardiography and effort intolerance in asymptomatic/minimally symptomatic patients with degenerative mitral regurgitation combined invasive –noninvasive hemodynamic monitoring. *Circ Cardiovasc Imaging* 2018;11:1–13.
14. AlJaroudi W, Alraies MC, Halley C, Rodriguez L, Grimm RA, Thomas JD, Jaber WA. Impact of progression of diastolic dysfunction on mortality in patients with normal ejection fraction. *Circulation* 2012;125:782–788.
15. Obokata M, Kane GC, Reddy YN V, Olson TP, Melenovsky V, Borlaug BA. Role of diastolic stress testing in the evaluation for heart failure with preserved ejection fraction. *Circulation* 2017;135:825–838.
16. Nagueh SF, Middleton KJ, Kopelen HA, Zoghbi WA, Quiñones MA. Doppler tissue imaging: a noninvasive technique for evaluation of left ventricular Relaxation and Estimation of Filling Pressures. *J Am Coll Cardiol* 1997;30:1527–1533.
17. Nagueh SF, Smiseth OA, Appleton CP, Byrd BF, Dokainish H, Edvardsen T, Flachskampf FA, Gillebert TC, Klein AL, Lancellotti P, Marino P, Oh JK, Alexandru Popescu B, Waggoner AD. Recommendations for the evaluation of left ventricular diastolic function by echocardiography: an update from the American Society of Echocardiography and the European Association of Cardiovascular Imaging. *Eur Hear J - Cardiovasc Imaging* 2016;17:1321–1360.
18. Haykowsky MJ, Brubaker PH, Morgan TM, Kritchevsky S, Eggebeen J, Kitzman DW. Impaired aerobic capacity and physical functional performance in older heart failure patients with preserved ejection fraction: Role of lean body mass. *J Gerontol - Ser A Biol Sci Med Sci* 2013;68:968–975.

19. Upadhyya B, Haykowsky MJ, Eggebeen J, Kitzman DW. Exercise intolerance in heart failure with preserved ejection fraction: More than a heart problem. *J Geriatr Cardiol* 2015;12:294–304.
20. Bertrand PB, Schwammenthal E, Levine RA, Vandervoort PM. Exercise dynamics in secondary mitral regurgitation. *Circulation* 2017;135:297–314.
21. Goliash G, Bartko PE, Pavo N, Neuhold S, Wurm R, Mascherbauer J, Lang IM, Strunk G, Hülsmann M. Refining the prognostic impact of functional mitral regurgitation in chronic heart failure. *Eur Heart J* 2018;39:39–46.